

Control Strategies and Digital Simulation of DFIG-based Wind Generators for Transient Stability Studies

Abstract. This paper presents the control strategies and digital simulation for the double-fed induction generator (DFIG)-based wind generators for transient stability studies. The wind turbine power tracking characteristics and the power flow mechanism of the DFIG-based wind plant are analyzed. The rotor-side converter (RSC) control, grid-side converter (GSC) control and the pitch angle control scheme are presented based on the phasor model of the DFIG system. The voltage-regulation mode and var-regulation mode are analyzed using control block diagram, and the simulation results of the benchmark system using Matlab/Simulink are presented. The voltage regulation mode and reactive power capabilities are found to be highly effective for low-voltage ride-through (LVRT) capabilities and transient stability enhancement of the DFIG-based wind generators.

Streszczenie. W artykule przedstawiono metodę sterowania silnika typu DFIG w zastosowaniu do elektrowni wiatrowej. Analizie poddano charakterystykę turbiny oraz obwodu mocy z maszyną. Zaprezentowano schematy blokowe zastosowanych struktur sterowania. Otrzymane wyniki symulacyjne potwierdziły wysoką skuteczność i stabilność proponowanego algorytmu także przy obniżonym napięciu sieci (LVRT). (Badanie algorytmu sterowania oraz badania symulacyjne maszyny DFIG w zastosowaniu do elektrowni wiatrowej).

Keywords: DFIG, wind generator, transient stability, voltage regulation, grid-integration, low-voltage ride through (LVRT)

Słowa kluczowe: DFIG, turbina wiatrowa, stabilność, regulacja napięcia, podłączenie do sieci, LVRT.

I. Introduction

In recent decades, the wind power are increasingly utilized for electric power generation and smart power applications. The integration of large wind farms into bulk power systems presents multiple challenges to system operation and security. One particular challenge to system security is vulnerability to common-mode tripping due to transmission system faults. Wind generators may have to be disconnected from the grid once the system has a disturbance, such as a short circuit fault, lightning strike on transmission lines, etc. With the increasing wind turbines in electric power generation the dynamic behavior of the power system is impacted considerably [1], [2].

Therefore, many electric utilities have issued grid codes to define the basic requirement concerning wind turbine behavior during grid faults. The focus in this relation is directed at the fault ride through (FRT) capability and the voltage support to be provided by the wind turbines during fault. Moreover, many wind farms, including large offshore projects, are geographically remote and have relatively weak transmission systems [2], [3].

The presence of wind farms in such weak systems raises serious concerns about system stability, voltage regulation, and post-fault power swings. During normal operation, wind farms should be capable of regulating voltage or reactive power to maintain a smooth voltage profile at the point of interconnection, protecting against voltage flicker caused by wind gusts. With the penetration of wind farms increasing, most utilities require that wind farms must tolerate system disturbances [4], [5].

This paper presents the control schemes and digital simulation for the double-fed induction generator (DFIG) wind generators for transient stability studies. The wind turbine power tracking characteristics and the power flow mechanism of the DFIG wind plant are analyzed. The control strategies of the DFIG wind generators are also presented, which consists of the rotor-side converter (RSC) control, grid-side converter (GSC) converter and the pitch angle control. The voltage regulation mode and var regulation mode are analyzed using control block diagram and the comparison of the simulation results. It is found that the voltage regulation mode and reactive support capabilities are highly effective for low-voltage ride-through (LVRT) capabilities and transient stability enhancement of the DFIG-based wind park.

II. DFIG-based Wind Power Generator

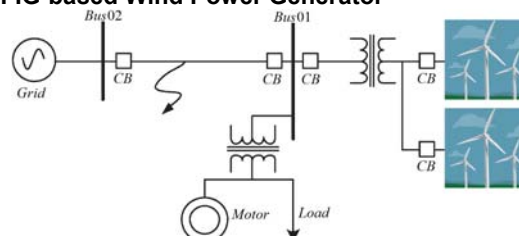


Fig.1 The diagram of the DFIG-based wind park

Fig.1 shows the diagram of the DFIG-based wind park, which consists of a six 1.5 MW wind turbines connected to a 35-kV distribution system exports power to a 110-kV grid through a 20-km, 35-kV feeder. A 2400V, 2-MVA plant consisting of a motor load (1.75 MW induction motor at 0.92 PF) and of a 300-kW resistive load is connected on the same feeder at bus Bus01. Both the wind turbine and the motor load have a protection system monitoring voltage, current and machine speed.

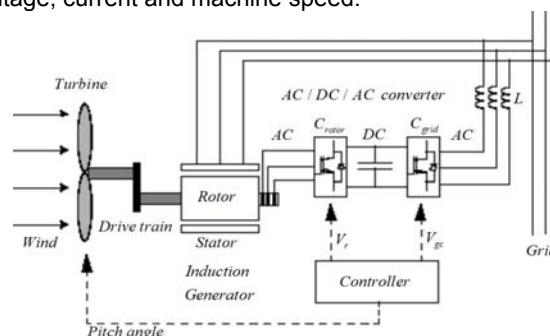


Fig.2 Circuit diagram of the DFIG wind generator

Fig.2 shows the circuit diagram of the DFIG wind generator, which consists of a wound rotor induction generator and an AC/DC/AC IGBT-based PWM converter. The stator winding is connected directly to the power grid while the rotor is fed at variable frequency through the AC/DC/AC converter. The DFIG technology allows extracting maximum energy from the wind for low wind speeds by optimizing the turbine speed, while minimizing mechanical stresses on the turbine during gusts of wind. The optimum turbine speed producing maximum mechanical energy for a given wind speed is proportional

to the wind speed. For wind speeds lower than 10 m/s the rotor is running at sub-synchronous speed. At high wind speed it is running at hyper-synchronous speed [3, 4, 5].

The model of the wind turbine is based on the steady-state power characteristics, where the stiffness of the drive train is infinite and the friction factor and the inertia of the turbine are combined with those of the generator coupled to the turbine. The output power of the turbine is given by the following equation:

$$(1) \quad P_m = c_p(\lambda, \beta) \frac{\rho A}{2} v_{wind}^3$$

where P_m denotes the mechanical output power of the turbine (W), $c_p(\lambda, \beta)$ denotes the performance coefficient of the turbine, ρ denotes the air density (kg/m³), A denotes the turbine swept area (m²), v_{wind} denotes the wind speed (m/s), λ denotes the tip speed ratio of the rotor blade tip speed to wind speed, and β denotes the blade pitch angle.

The mechanical power P_m as a function of generator speed, for different wind speeds and for blade pitch angle $\beta=0$ degree, is illustrated in Fig.3. This figure is obtained with the parameters: base wind speed=12 m/s, maximum power at base wind speed=0.73 pu and base rotational speed=1.2 pu.

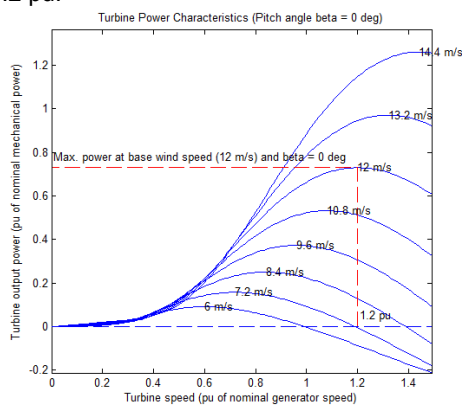


Fig.3 Turbine power tracking characteristic

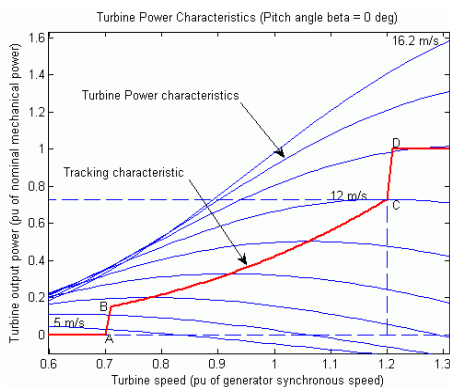


Fig.4 Enlarged view of the turbine power tracking characteristic

Fig.4 shows the turbine power tracking characteristic, by the ABCD curve superimposed to the mechanical power characteristics of the turbine obtained at different wind speeds. The turbine mechanical power as function of turbine speed is displayed for wind speeds ranging from 5 m/s to 16.2 m/s. The DFIG is controlled in order to follow the red curve. The advantage of the DFIG technology is the ability for power electronic converters to generate or absorb reactive power, thus eliminating the need for installing capacitor banks as in the case of squirrel-cage induction generators.

The actual speed of the turbine ω_r is measured and the mechanical power of the tracking characteristic is used as

the reference power for the power control loop. The tracking characteristic is defined by four points: A, B, C and D. From zero speed to speed of point A the reference power is zero. Between point A and point B the tracking characteristic is a straight line, the speed of point B must be greater than the speed of point A.

Between point B and point C the tracking characteristic is the locus of the maximum power of the turbine (maxima of the turbine power vs turbine speed curves). The tracking characteristic is a straight line from point C and point D. The power at point D is one per unit (1 pu) and the speed of the point D must be greater than the speed of point C. Beyond point D the reference power is a constant equal to one per unit.

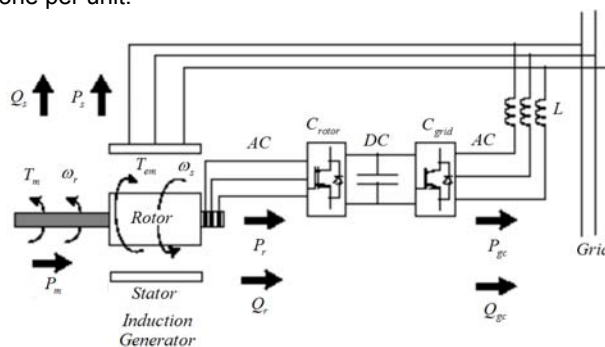


Fig.5 The illustration of power flow of the DFIG wind generator

Fig.5 shows the illustration of power flow of the DFIG wind generator. The term P_m denotes the mechanical power captured by the wind turbine and transmitted to the rotor, P_s and P_r denote the stator and rotor electrical power output, respectively. The terms P_{gc} and Q_{gc} denote the active and reactive power output of the grid side converter (GSC). The terms Q_s and Q_r denote the stator and rotor reactive power output.

The terms T_m and T_{em} denote the mechanical and electromagnetic torque applied to the rotor. The absolute value of slip ($s=1-\omega_r/\omega_s$) is much lower than 1 and, consequently, P_r is only a fraction of P_s . Since T_m is positive for power generation and ω_s is positive and constant for a constant frequency grid voltage, the sign of P_r is a function of the slip sign. P_r is positive for negative slip (speed greater than synchronous speed) and it is negative for positive slip (speed lower than synchronous speed).

For super-synchronous speed operation, active power P_r is transmitted to DC bus capacitor and tends to rise the DC voltage. For sub-synchronous speed operation, P_r is taken out of DC bus capacitor and tends to decrease the DC voltage. The grid side converter (GSC) C_{grid} is used to generate or absorb the power P_{gc} in order to keep the DC voltage constant. In the steady-state conditions, P_{gc} is equal to P_r for a lossless AC/DC/AC converter, and the speed of the wind turbine is determined by the power P_r absorbed or generated by the rotor side converter C_{rotor} .

The phase-sequence of the AC voltage generated by C_{rotor} is positive for sub-synchronous speed and negative for super-synchronous speed. The frequency of the voltage is equal to the product of the grid frequency and the absolute value of the slip. The rotor side and grid side converters C_{rotor} and C_{grid} have the capability of generating or absorbing reactive power and can be used to control the reactive power or the voltage at the grid terminals

III. Control Scheme for the Rotor-side Converter

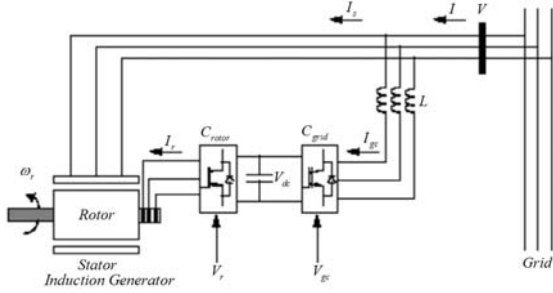


Fig.6 Diagram of the DFIG wind generator for controller design

Fig.6 shows the diagram of the DFIG wind generator for control design purposes. The rotor-side converter (RSC) is used to control the wind turbine output power and the voltage (or reactive power) measured at the grid terminals. The control block diagram of the RSC is shown in Fig.7.

A. Active Power Control

The actual electrical output power, measured at the grid terminals of the wind turbine, is added to the total power losses (mechanical and electrical) and is compared with the reference power P_{ref} obtained from the tracking characteristic. A proportional-integral (PI) regulator is used to reduce the power error to zero. The output of this regulator is the reference rotor current $I_{qr,ref}$ that must be injected in the rotor by converter C_{rotor} .

This is the current component that produces the electromagnetic torque T_{em} . The actual positive-sequence current component I_{qr} is compared to $I_{qr,ref}$ and the error is reduced to zero by a current regulator (PI). The output of this current controller is the voltage V_{qr} generated by C_{rotor} . The current regulator is assisted by feed forward terms which predict V_{qr} .

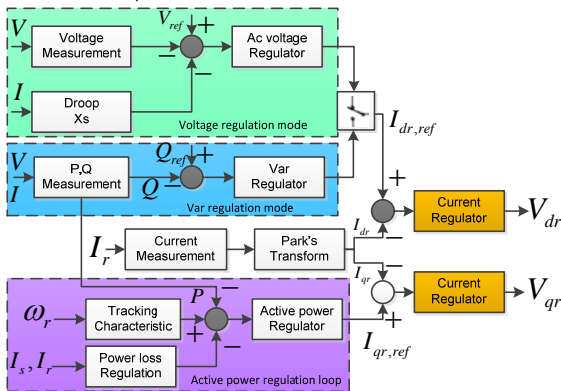


Fig.7 Control block diagram of the rotor-side converter (RSC)

B. Voltage Regulation Mode

The voltage or the reactive power at grid terminals is controlled by the reactive current flowing in the converter C_{rotor} . When the wind turbine is operated in voltage regulation mode, it implements the following *V-I characteristic*, as shown in Fig.8.

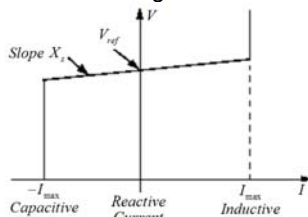


Fig.8 Wind turbine V-I characteristic

As long as the reactive current stays within the maximum current values ($-I_{max}$, I_{max}) imposed by the

converter rating, the voltage is regulated at the reference voltage V_{ref} . However, a voltage droop is normally used (usually between 1% and 4% at maximum reactive power output). In the voltage regulation mode, the *V-I characteristic* is described by the following equation:

$$(1) \quad V = V_{ref} + X_s I$$

where V denotes the positive sequence voltage (*pu*), I denotes the reactive current (*pu/P_{nom}*) ($I > 0$ indicates an inductive current), X_s denotes the slope or droop reactance (*pu/P_{nom}*), P_{nom} denotes the three-phase nominal power of the converter.

C. Var Regulation Mode

When the wind turbine is operated in *var* regulation mode the reactive power at grid terminals is kept constant by a *var* regulator. The output of the voltage regulator or the *var* regulator is the reference *d*-axis current $I_{dr,ref}$ that is injected in the rotor by converter C_{rotor} . The same current regulator as for the power control is used to regulate the actual I_{dr} component of positive-sequence current to its reference value. The output of this regulator is the *d*-axis voltage V_{dr} generated by the rotor side converter C_{rotor} .

IV. Control Scheme for the Grid-side Converter

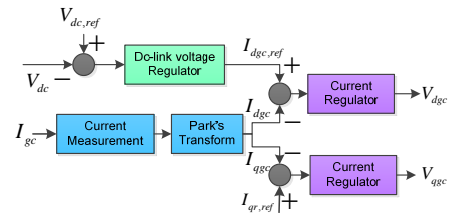


Fig.9 The control diagram of the grid side converter (GSC)

The grid side converter (GSC) C_{grid} is used to regulate the voltage of the DC bus capacitor. And it can also be controlled to generate or absorb reactive power. Fig.8 shows the control block diagram of the grid side converter, which consists of the measurement systems to detect the *d* and *q* components of AC positive-sequence currents to be controlled as well as the DC voltage V_{dc} .

Besides, an outer regulation loop consisting of a DC voltage regulator. The output of the DC voltage regulator is the reference current $I_{dgc,ref}$ for the current regulator (I_{dgc} = current in phase with grid voltage which controls active power flow). The current regulator controls the magnitude and phase of the voltage generated by converter C_{grid} (V_{gc}) from the $I_{dgc,ref}$ produced by the DC voltage regulator and the specified $I_{q,ref}$ reference.

V. Pitch-Angle Control System

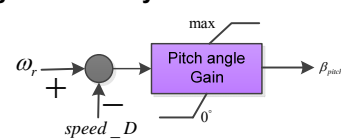


Fig.10 The block diagram of the pitch angle controller

Fig.10 shows the block diagram of the pitch angle controller. The pitch angle is kept constant at zero degree until the speed reaches the point D speed of the tracking characteristic. Beyond the point D the pitch angle is proportional to the speed deviation from point the D speed [see Fig.4].

VI. Case Study of the Target System

This section presents the simulation results of the DFIG-based wind park. The parameters are consistent with Section II. Fig.11 shows the simulation results of the DFIG-

wind plant under abrupt increase of wind speed from 8m/s to 14m/s. Initially, wind speed is set at 8 m/s, then at $t=5s$, wind speed increases suddenly at 14 m/s at $t=10s$. The generated active power starts to increase smoothly (together with the turbine speed) to reach its rated value of 9 MW in approximately 15 s. Over that time frame the turbine speed increases from 0.8 pu to 1.21 pu.

Besides, the pitch angle of the turbine blades is zero degree initially and the turbine operating point follows the red curve of the turbine power characteristics up to point D. Then the pitch angle is increased from 0 deg to 0.76 deg in order to limit the mechanical power. The reactive power is controlled to maintain a constant terminal voltage. At nominal power, the wind turbine absorbs 0.68 Mvar (generated $Q = -0.68$ Mvar) to control voltage at 1pu.

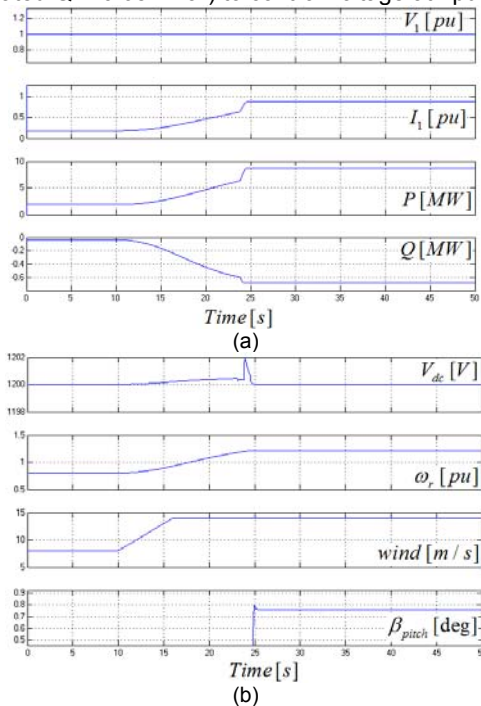


Fig.11 Simulation results of the DFIG-wind plant under abrupt increase of wind speed from 8m/s to 14m/s. (a).The positive-sequence fundamental component voltage and current and the active power, reactive power of the wind power plant. (b).The dc-link voltage, angular speed of DFIG generator and wind speed, pitch angle of the wind turbine.

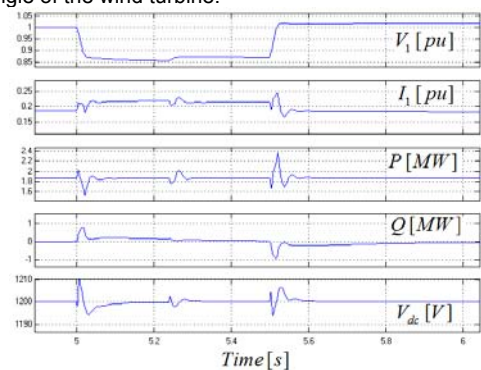


Fig.12 Simulation results of the DFIG-wind plant under remote fault using var regulation mode (0.15pu voltage sag occurs at the high voltage grid).

Fig.12 shows the simulation results of the DFIG-wind plant under remote fault using var regulation mode (0.15pu voltage sag occurs at the high voltage grid). From Fig.12, it shows that the voltage falls below 0.9 pu and at $t = 5.22$ s, the protection system trips the plant since an under-voltage lasting more than 0.2 s has been detected. The plant current falls to zero and motor speed decreases gradually,

and the wind farm continues generating at a power level of 1.87 MW. After the plant has tripped, 1.25 MW of power is exported to the grid.

Fig.13 shows the simulation results of the DFIG-wind plant under remote fault using voltage regulation mode. It is found that the plant does not trip anymore due to the voltage support provided by the 5 Mvar reactive-power generated by the wind-turbines during the voltage sag, which keeps the plant voltage above the 0.9 pu protection threshold. The plant voltage during the voltage sag is now 0.93 pu.

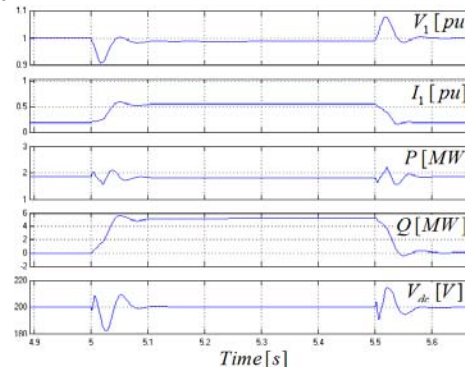


Fig.13 Simulation results of the DFIG-wind plant under remote fault using voltage regulation mode (0.15pu voltage sag occurs at the high voltage grid)

VII. Conclusions

This paper presents the principles and control schemes for the double-fed induction generator (DFIG)-based wind park. The wind turbine power tracking characteristics, the power flow mechanism and the control strategies of the DFIG wind plant are presented. The voltage regulation mode and var regulation mode are analyzed using control block diagram, and a comparison of the simulation results is also presented. It is found that the voltage regulation mode and reactive support capabilities are highly effective for low-voltage ride-through (LVRT) and transient stability enhancement of the DFIG wind park.

Acknowledgment

This project is supported by the Fundamental Research Funds for the Central Universities of China under grant (ZYGX2011J093).

REFERENCES

- [1] Y. Zhou, P. Bauer, J. A., Ferreira, J. Pierik, Operation of grid-connected DFIG under unbalanced grid voltage condition, *IEEE Trans. on Energy Convers.*, 24(2009), n.1, 240-246.
- [2] R. Pena, R. Cardenas, J. Clare, and P. Wheeler, Control system for unbalanced operation of stand-alone doubly fed induction generators, *IEEE Trans. Energy Convers.*, 22(2007), n.2, 544-545.
- [3] A. Petersson, T. Thiringer, L. Harnefors, and T. Petru, Modelling and experimental verification of grid interaction of a DFIG wind turbine, *IEEE Trans. Energy Convers.*, 20(2005), n.4, 878-886.
- [4] S. Seman, J. Niiranen, and A. Arkkio, Ride-through analysis of doubly fed induction wind-power generator under unsymmetrical network disturbance, *IEEE Trans. Power Syst.*, 21(2006), n.4, 1782-1789.
- [5] M. Cheng, X. Cai, G. Wu, Investigation of transient torque during a power system fault in wind power turbines having a DFIG and crowbar circuit, *Przeglad Elektrot.*, 87(2011), n.11, 245-250.

Author: Dr. Yang Han is with the Department of Power Electronics, School of Mechanical, Electronic, and Industrial Engineering, University of Electronic Science and Technology of China (UESTC), No.2006 XiYuan Road, Chengdu, China, 611731, E-mail: hanyang_facts@hotmail.com, hanyang@uestc.edu.cn